Use of unresolved transition arrays for plasma diagnostics

A. Zigler, M. Givon, E. Yarkoni, M. Kishinevsky, E. Goldberg, and B. Arad
Department of Plasma Physics, Soreq Nuclear Research Center, 70 600 Yavne, Israel

M. Klapisch
Racah Institute of Physics, The Hebrew University of Jerusalem, 91 904 Jerusalem, Israel
(Received 24 June 1986)

The use of unresolved transition arrays for the determination of plasma temperature is described. A compact low-resolution spectrometer, based on this technique, which yields both temporally and spatially resolved data, has been constructed. It may be developed easily into a real-time device.

I. INTRODUCTION

Experimental spectroscopy data of multiply-charged ions are used in order to study the basic processes which occur in hot plasmas. Various methods have been developed[1] for the determination of the plasma composition and the fractional abundance of the various ionic species, as well as the plasma temperature and density. All these methods are based on the interpretation of H-like and He-like spectra emitted by ions of low and medium Z elements. They require high-resolution measurements of the ratios between the intensities of various satellites and intercombination lines and those of the resonance lines. Since most of the above-mentioned spectra are em-

TABLE I. Spatially resolved lanthanum intensities of (I)[a] grouped into various bands.

Ion bands	Distance (μm)	Total intensity	$\frac{I_{\geq 150}}{I_{\geq 30}} \times 100$	Corrected intensity	$\frac{I_{\geq 150}}{I_{\geq 30}} \times 100$
Ni-like	30	3.00		0.38	
			40%		65%
	150	1.2		0.25	
	300	1.0		0.1	
Co-like	30	9.8		0.7	
			50%		85%
	150	4.8		0.61	
	300	3.8		0.52	
Fe-like	30	7.5		0.98	
			55%		95%
	150	4.0		0.94	
	300	2.6		0.52	
Mn-like	30	5.9		0.46	
			35%		85%
	150	2.1		0.38	
	300	1.6		0.23	
Cr-like	30	3.9		0.39	
			60%		85%
	150	2.3		0.33	
	300	1.5		0.2	
V-like	30	2.7		0.28	
			60%		80%
	150	1.8		0.23	
	300	0.7		0.05	

[a]Intensity at x micrometers is the total plume intensity at a distance of x micrometers away from the target and outward.

itted in the x-ray region, they are recorded by crystal diffraction spectrometers of various designs. In all these spectrometers the necessary high resolution is obtained by increasing the distance between the source and the diffracting crystal. This increase in resolution is obtained at the expense of the photon flux. Low flux makes measurements with high space and time resolution impossible.

In this paper we propose the use of complex high-Z element spectra for the purpose of plasma diagnostics. These spectra consist of large numbers of unresolved lines belonging to the same unresolved transition arrays (so-called UTA).[2] In the present method only the various arrays have to be resolved and hence the required resolution is low. Low spectral resolution can be obtained using small geometrical dimensions. These features make high photon fluxes possible and consequently the measurement can be carried out with high spatial or temporal resolution, or with both spatial and temporal resolution.

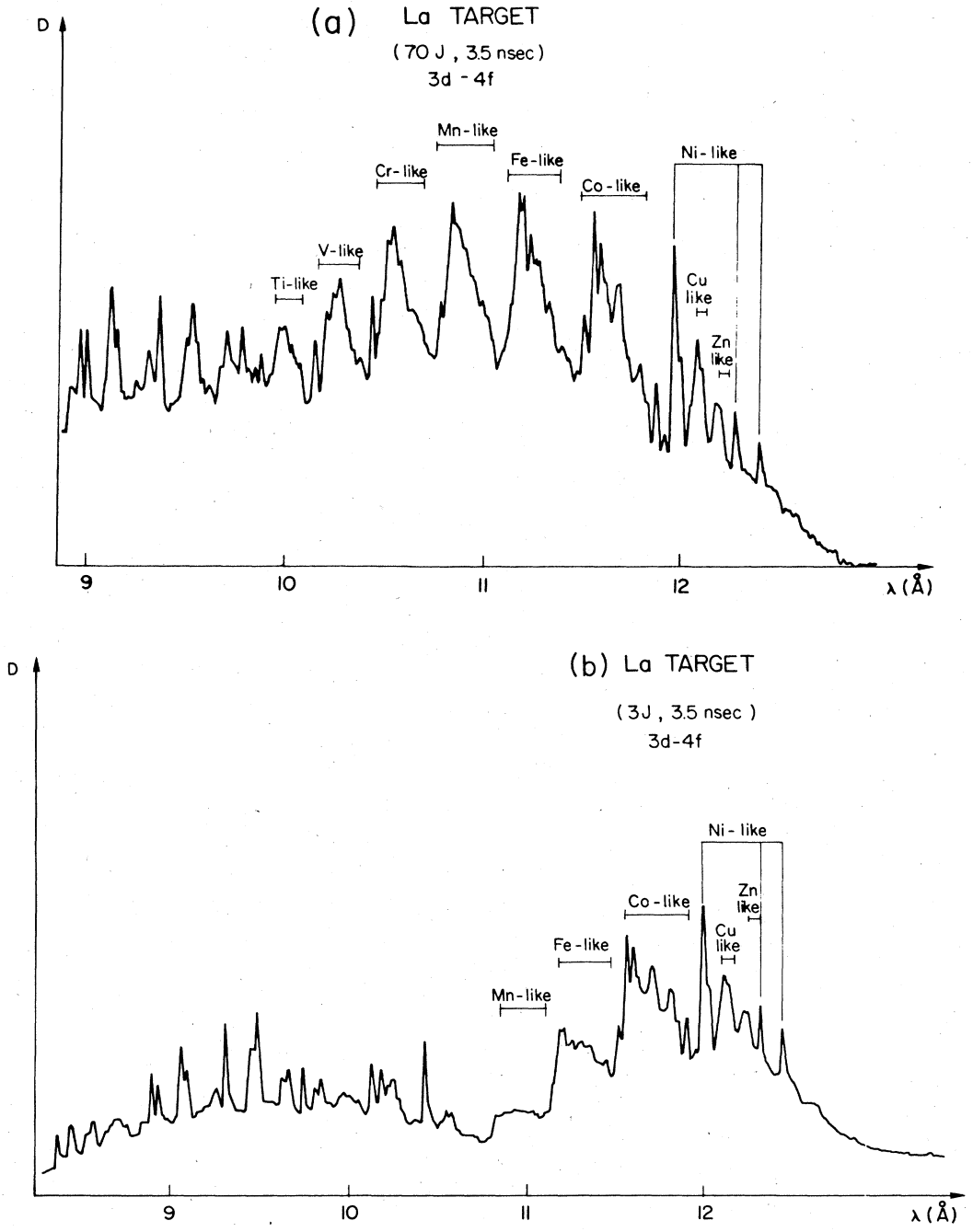

FIG. 1. X-ray spectra of laser-produced plasma from a lanthanum target.

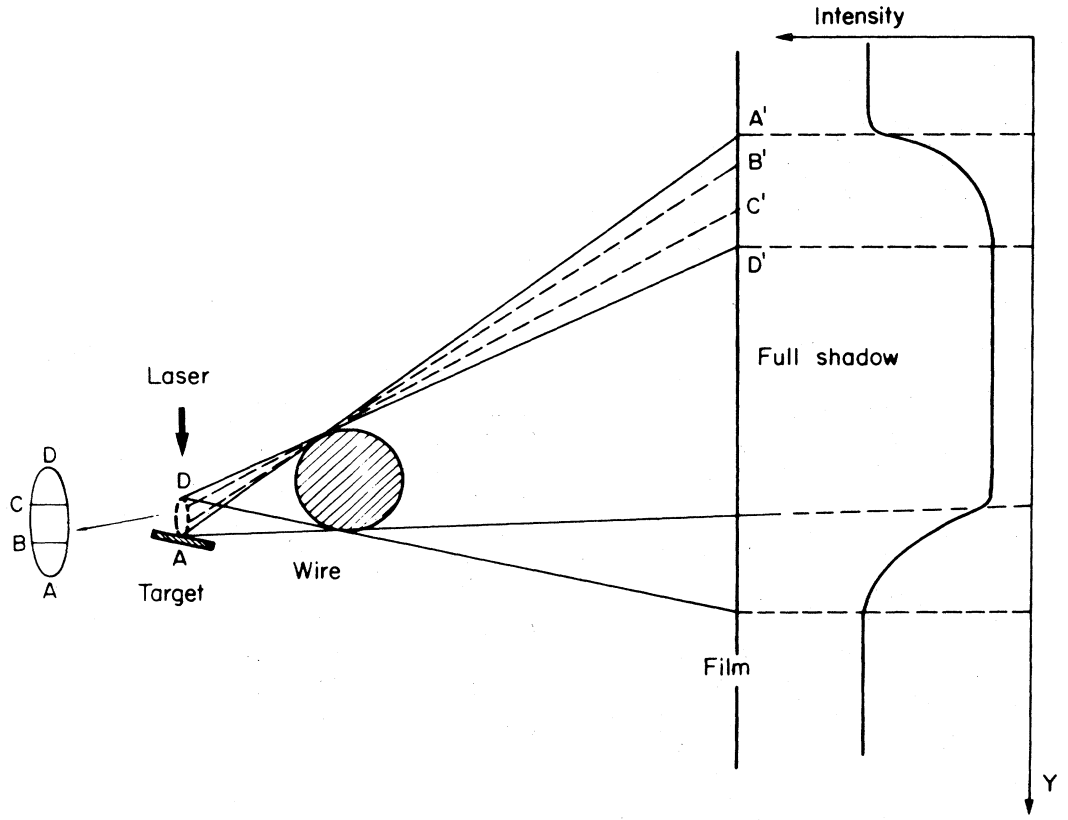

FIG. 2. Schematic representation of the shadow technique for obtaining spatial resolution.

II. THEORETICAL BACKGROUND

The x-ray spectrum of a hot-Z element plasma is characterized by wide bands of transitions, where each band belongs to a different isoelectronic sequence. A reliable theory is required in order to be able to use these bands for plasma diagnostics. As can be seen from Fig. 1, the spectra include isolated peaks. Most of these peaks correspond to transition arrays that consist of numerous closely packed lines. Thus it is clear that detailed line calculations cannot be a satisfactory way of identifying these spectra. To do this, a model describing the unresolved transition array (UTA) as a whole was developed.[2] In this model, the arrays were described as intensity-weighted distributions of transition energies, and simple analytical expressions for the mean and the variance of the weighted distribution were developed. However, in many cases of highly ionized heavy atoms, the spin-orbit splitting of one (or several) electrons is the dominant feature of the configuration, so that the transition array actually splits into

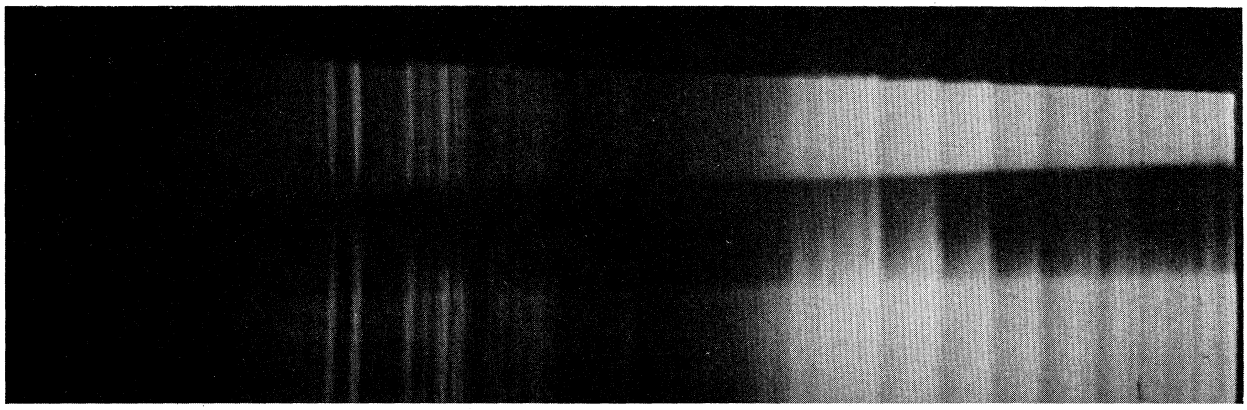

FIG. 3. Spatially resolved x-ray spectrum of a laser-produced praseodymium plasma.

nearly pure jj well-separated subarrays. For these cases the UTA model was extended[9] to give the first and the second moments (mean energy and variance) of each of the spin-orbit split subarrays. We shall refer to this as the spin-orbit-split array (SOSA) model.

The SOSA model has recently been applied to the identification of $3d$-$4f$ transitions in the x-ray spectra of highly ionized (Ge-like—Co-like) Tm—Re (Ref. 3) and $3d$-$5f$, $6f$ transitions in tungsten and gold[4] in laser-produced plasma, showing excellent agreement with experiment. Thus, it can be seen that the UTA model provides a useful tool for plasma diagnostics.

III. EXPERIMENTAL AND RESULTS

Figure 1 shows two laser-produced lanthanum spectra obtained at the Soreq Nuclear Research Center Nd-glass laser facility. The laser energy varied between 3 and 70 J, while the laser Gaussian pulse shape of 3.5 nsec full width at half maximum (FWHM) was kept constant. The beam was focused by a lens onto plane targets. The x-rays were dispersed by a potassium ammonium phosphate (KAP) crystal and recorded on RAR 2495 film. The recorded spectrum was processed by a computerized microdensitometer. The energies were calibrated using known reference spectra, and the intensities were obtained from the known film response.[5] In order to be able to properly interpret spectra such as shown in Fig. 1, the same spectra were also recorded with spatial resolution. Although this technique has been published previously[6] we shall outline its main features in order to better understand the plasma diagnostics described here.

Figure 2 is a schematic description of the partial shadow method. The small ellipse touching the target represents the plasma profile. The circle represents a wire which casts a shadow on the film. Both plasma and wire are highly exaggerated in the figure. Obviously, before reaching the film, the x rays hit a dispersive crystal (not shown in the figure). The crystal, however, disperses, according to wavelength, only in one direction while in the perpendicular direction there is no wavelength dependence, and this is the direction in which the shadow is cast. The region on the film extending from the solid line and outward (from A' and up in the figure) is irradiated by all of the plasma. The region on the film between the solid and broken lines ($A'B'$) is irradiated by most of the plasma, except the dense and cool region close to the target (AB). When we approach D' (the edge of the full shadow), the film is affected by smaller and smaller regions of the plasma (CD), until finally the region close to D' is irradiated only by the hot, low-density corona. When the distances between the target and the wire, and between the wire and the film are known accurately, the plasma region affecting a certain point on the film can be calculated. Figure 3 is a print of a spatially resolved x-ray spectrum of praseodymium, which shows clearly the full and partial shadows in the various UTA's. Figure 4 shows four laser-produced x-ray spectra of lanthanum as emitted in various parts of the plasma: from the denser part of the plasma at 30 μm from the target, to the outer part of the corona at 300 μm.

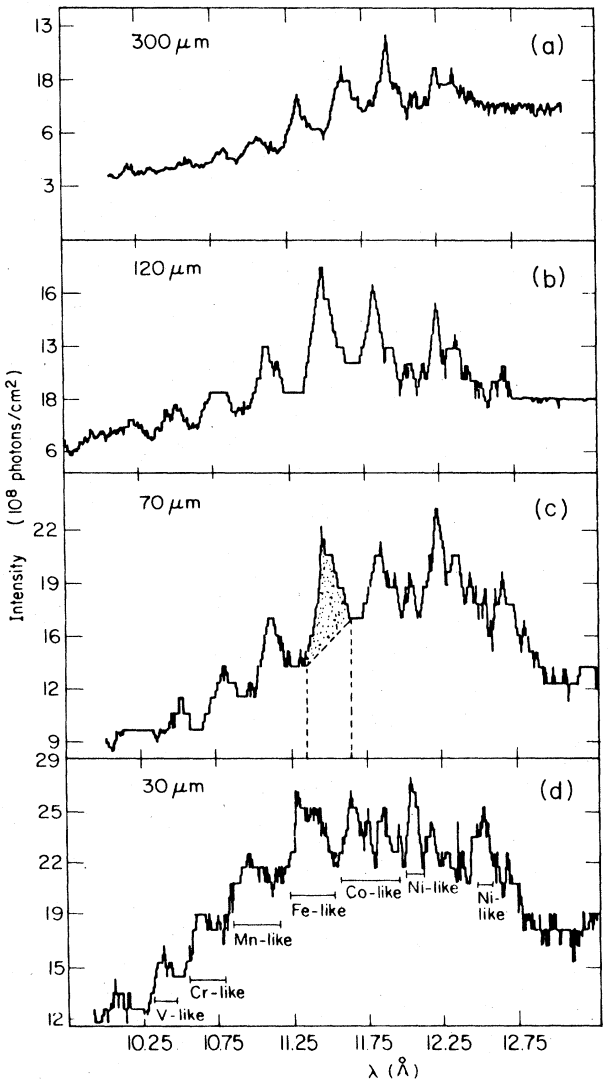

FIG. 4. X-ray spectra of laser-produced lanthanum plasma. Each spectrum is obtained from that part of the plasma which starts at a distance of Y μm from the target and extends outward. Distance Y for each spectrum is marked on the left of it.

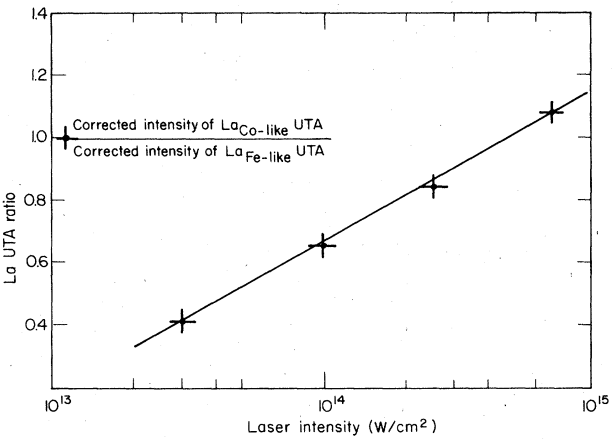

FIG. 5. Plot of the intensity ratio of the Fe-like UTA to the Co-like UTA as a function of the laser irradiance.

We define two intensities. The total band intensity includes the whole area between the graph and the wavelength axis, while the corrected intensity is the same area from which the semicontinuum is subtracted (the dotted area). Table I summarizes the total and corrected intensities as a function of the distance from the target for the various UTA's of Fig. 4. The percentages are the ratios between the intensities due to the part of the plasma $>150\ \mu$m from the target, and those due to the part of the plasma $>30\ \mu$m from the target.

As described previously, the spectrum recorded 150 μm away from the target originates mainly in the hot corona. The high percentages in the last column of the table, as compared with those in the fourth, show clearly that the corrected intensity describes the intensity of the UTA contributed by the outer corona of the plasma. Therefore, the band structure mainly represents the emission from the corona. Thus the space integrated spectrum may be

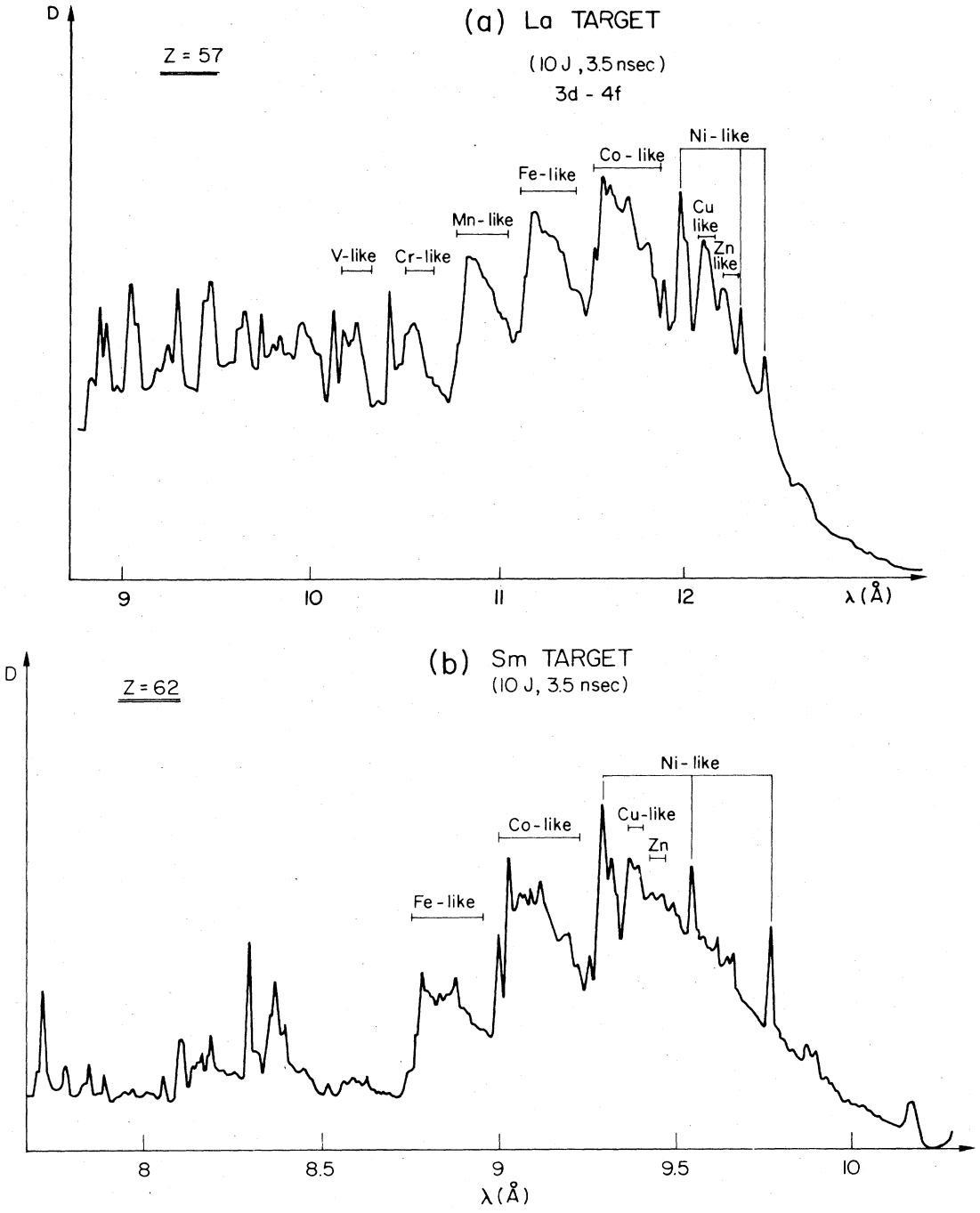

FIG. 6. X-ray spectra of laser-produced plasma of lanthanum ($Z=57$) and samarium ($Z=62$). Laser energy and intensity were kept constant.

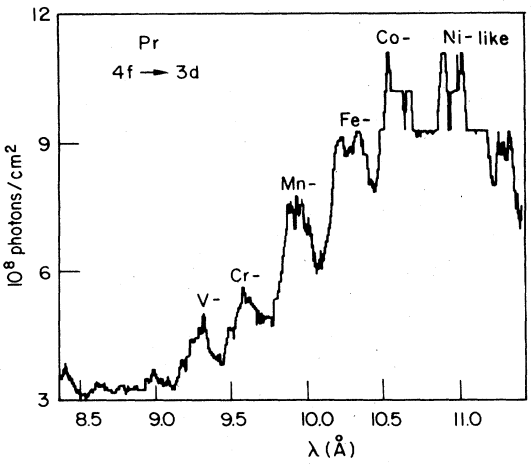

FIG. 7. X-ray spectrum of laser-produced praseodymium plasma as recorded by the compact spectrometer.

used for the determination of laser plasma parameters. In the spectrum of lanthanum produced by a laser pulse of 3 J (Fig. 1), the Mn-like UTA can hardly be observed, whereas in the spectrum produced by a 70 J pulse, UTA's as far as Ti-like are clearly distinguished. Figure 5 shows a plot of the intensity ratio of two neighboring UTA's as a function of the laser intensity. Since the temperature of the laser-produced plasma is a function of the laser intensity,[7,8] the plot of Fig. 5 can be used for temperature determination after proper calibration.

The sensitivity of the method is demonstrated by the following results. Figure 6 shows spectra of lanthanum and samarium produced by two laser pulses of identical energy and specific power. The effective charges (Z) of the two elements differ by only 10% and since the ionization potential is proportional to Z^2, we may assume similar electron densities. Since the relative population of the various UTA's is a function of electron density, ionization potential, and electron temperature, the main factor which determines differences in the populations of these two elements is the electron temperature. The great difference between the two spectra shows clearly the sensitivity of the UTA method to changes in electron temperature.

Figure 7 shows a $3d$-$4f$ UTA spectrum of praseodymium obtained at a laser energy of 5 J with a convex KAP crystal which is included in a small spectrometer. This spectrometer was constructed by us with overall dimensions of $5\times3\times1$ cm^3. One can see from the figure that the various bands are easily distinguishable.

IV. SUMMARY AND CONCLUSIONS

We have shown here that UTA spectroscopy of high-Z elements yields valuable information regarding hot plasma parameters. Using the SOSA model, the band calculation and identification of the ionization stages is very reliable, making UTA spectroscopy an efficient tool for plasma diagnostics. Furthermore, unlike line spectroscopy which requires a high resolution of $\lambda/\Delta\lambda\sim1000$ or better, UTA spectroscopy needs only to discriminate between the various bands, and hence low resolution of $\lambda/\Delta\lambda\sim50$ is sufficient. Because of the low resolution required, the spectra can be recorded in a compact spectrometer which can be placed close to the plasma. Such a spectrometer has been constructed with small dimensions as described above and has been found to meet the above-mentioned requirements.

The compact spectrometer has several advantages. The small size of the recording film enables one to replace it directly with a two-dimensional diode array, thus obtaining the information on a real-time basis. Furthermore, compactness is of great advantage for tokomak plasma diagnostics where the spectrometer can be placed close to the first wall and not far away, as is the case with most spectrometers. This arrangement will enable one to obtain time-dependent information with high statistical accuracy.

In conclusion, a method for the reduction of plasma parameters, using low-resolution spectroscopy of UTA's, has been described which has the following advantages: (1) the spectrometer itself can be made small and of low resolution; (2) high spatial and time resolution is obtainable; (3) due to the simplicity of the physical principles involved, data reduction is simplified; (4) last but not least, the device is of low cost.

ACKNOWLEDGMENTS

The authors would like to thank R. Laluz, S. Mamam, and Y. Sapir for their technical assistance in the experiments. This work was partially supported by a grant of the U.S.-Israel Binational Science Foundation, No. 84-00207.

[1] *Plasma Diagnostics,* edited by W. Lochte-Holtgreven (North-Holland, Amsterdam, 1968).

[2] C. Bauche-Arnoult, J. Bauche, and M. Klapisch, Phys. Rev. A **20**, 2424 (1979); **25**, 2641 (1982); **30**, 3026 (1984); M. Klapisch, E. Meroz, P. Mandelbaum, and A. Zigler, *ibid.* **25**, 2391 (1982).

[3] M. Klapisch, P. Mandelbaum, A. Zigler, C. Bauche-Arnoult, and J. Bauche, Phys. Scr. **34**, 51 (1986).

[4] A. Zigler, M. Klapisch, and P. Mandelbaum, Phys. Lett. A **117**, 31 (1986); C. Bauche-Arnoult, E. Luc-Koening, J. F. Wyart, J. P. Geindre, P. Audebert, P. Monier, J. C. Gauthier, and C. Chesnais-Popovics, Phys. Rev. A **33**, 791 (1986).

[5] C. M. Dozier, D. B. Brown, L. S. Birks, P. B. Lyons, and R. F. Benjamin, J. Appl. Phys. **47**, 3732 (1976). B. L. Henke, F. G. Fujiwara, M. A. Tester, C. H. Dittmore, and M. A. Palmer, J. Opt. Soc. Am. B **1**, 828 (1984)

[6] A. Zigler, H. Zmora, and Y. Komet, Phys. Lett., **60A**, 319 (1977).

[7] M. H. Key, in *Laser Plasma Interaction,* edited by R. A. Cairns and J. J. Sanderson (Scottish University Summer School, 1980), Eq. (3.16), p. 236.

[8] C. E. Max, University of California Report No. UCRL-53107, 1981 (unpublished).

[9] C. Bauche-Arnoult, J. Bauche, and M. Klapisch, Phys. Rev. A **31**, 2248 (1985).

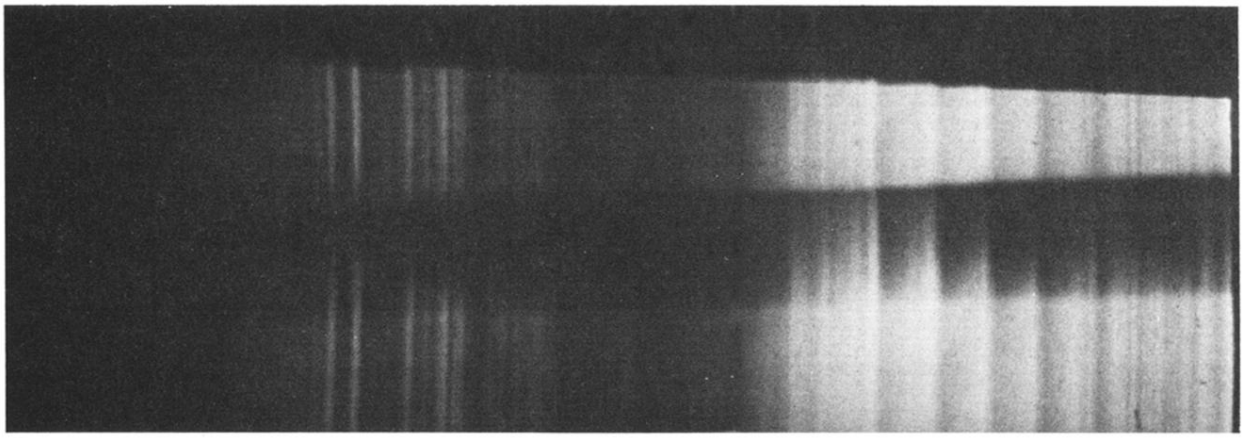

FIG. 3. Spatially resolved x-ray spectrum of a laser-produced praseodymium plasma.